Transport Properties of the Semiconductor Superlattice

Abstract: Precise calculations have been made, by Monte Carlo methods, of electron transport properties of the Esaki superlattice. The calculations were on a single-particle space-homogeneous basis, with a model of the superlattice which could be reasonably close to reality. Steady-state longitudinal drift-velocity/field characteristics were obtained, for four sets of parameter values; they exhibited the expected maximum followed by negative differential mobility. The accompanying variations of the longitudinal and transverse energy averages were also obtained, and the distribution functions for longitudinal wavevector and transverse energy were investigated. The frequency dependences of the differential mobilities (in-phase and out-of-phase components) were obtained in some representative cases; they exhibited a "Bloch resonance."

1. Introduction

Esaki, et al. [1] have proposed a semiconductor material in which the electrons would move in a potential varying periodically, in one dimension, on a scale of many lattice constants; and have recently fabricated samples [2] of gallium aluminum arsenide alloy in which the aluminum fraction (the "x" of Ga_{1-x}Al_xAs) was made to vary periodically by controlling the growth chemistry. The idea [1] is that the superlattice potential-in this case the band-edge energy, considered as a function of position - would cause a kind of Bloch band structure superposed on that due to the lattice-periodic forces. The former would have a smaller Brillouin zone size, and in practice a narrower energy scale of bands and gaps. Because the superlattice potential is to be one dimensional, these "superbands" should, in the lower part of the conduction band, be separated by forbidden energy ranges.

An intuitively perceived consequence of this situation is that the electron drift velocity would reach a maximum, with increasing electric field, followed by a field range with negative differential mobility. A second intuition is that the response to an added periodically timevarying field should exhibit a resonance when the period is equal to the time for an electron subject to the static electric field to cross the Brillouin superzone. It is demonstrated in the present paper that both of these expectations are correct.

The viewpoint of the present work is to take the simplest model that should contain the essential features of superlattice material, disregarding further detail which is, in any case, not likely to be explicitly known or calculable at this stage, and make precise calculations of its transport properties over a significant range of parameter values.

2. Formulation

It is implicit in the conceptions used [1] that an electron may be assigned a wavevector, in the superzone, which will vary with position and time. It is, accordingly, necessary that the electron mean free path be at least several superlattice constants [3]. This condition has evidently been at least fairly well satisfied [2]. Then the state of the electrons may be represented by a Boltzmann equation, for a superzone distribution function $f(\mathbf{k})$:

$$\frac{\partial}{\partial t} f = -\frac{e}{\hbar} \, \mathcal{E} \cdot \frac{\partial}{\partial \mathbf{k}} f
+ \int d^3 \mathbf{k}' \, \left[f(\mathbf{k}') W(\mathbf{k}', \mathbf{k}) - f(\mathbf{k}) W(\mathbf{k}, \mathbf{k}') \right], \tag{1}$$

where the electric field is \mathscr{E} , and for convenience the carrier charge is taken as positive (+e).

Equation (1) embodies the assumption that the electrons are confined to a single superband—in particular, the lowest one—which is to be examined subsequently. The scattering term on the right does not include carrier-carrier interactions. The drift velocity is the average value

39

$$\mathbf{u} = \langle \mathbf{v} \rangle \equiv \int d^3 \mathbf{k} f(\mathbf{k}) \mathbf{v}(\mathbf{k}) \tag{2}$$

of the electron velocity

$$\mathbf{v}(\mathbf{k}) = \frac{1}{\hbar} \frac{\partial E}{\partial \mathbf{k}}.\tag{3}$$

In (3), E is the superband energy, for which (neglecting effects of dependence of the band effective mass on the concentration x) we take

$$E(\mathbf{k}) = E_1(k_{11}) + E_2(k_{\perp}) , \qquad (4)$$

where $k_{||}$ and k_{\perp} are the components parallel and perpendicular to the superlattice axis, E_1 has the reciprocallattice periodicity, and

$$E_2(k_\perp) = (\hbar^2/2m^*)k_\perp^2. \tag{5}$$

It is assumed here that $\mathscr E$ is parallel to the superlattice axis (the $k_{||}$ direction).

The foregoing scheme can be seen, from simple considerations, to require the anticipated negative differential mobility. For small enough constant \mathcal{E} , we must have the ohmic relation $u = \mu_0 \mathcal{E}$. For large enough \mathcal{E} , on the other hand, we expect f and u to be given by a series in inverse powers of \mathcal{E} . Then it follows from (1) that the first term for f is independent of k_{11} :

$$f(\mathbf{k}) \approx g(k_{\perp})$$
, (6)

where the function g is determined by the vanishing of the scattering term (with kernel W integrated over $k_{||}$ and $k_{||}'$). Then, in the same limit, it follows from (6) that u=0. To get the next term in u, proportional to $1/\varepsilon$, explicitly one may substitute from (6) in the right-hand side of the "energy conservation equation"

$$eu\varepsilon = \langle w \rangle \equiv \int wf \, d^3\mathbf{k} \,,$$
 (7)

where

$$w(\mathbf{k}) \equiv \int W(\mathbf{k}, \mathbf{k}') \left[E(\mathbf{k}) - E(\mathbf{k}') \right] d^3 \mathbf{k}'. \tag{8}$$

It is now obvious that $u(\mathcal{E})$ must pass through a maximum, between the limiting forms $\mu_0 \mathcal{E}$ and const/ \mathcal{E} . One should note that the foregoing argument depends on the fact that E_1 is bounded above, and, thus, on the related restriction of the electrons to a single band. Consequently, the critical issue, in practice, may be whether the function g in (6) corresponds to there being, or not being, an appreciable fraction of the electrons with E_2 values high enough for them to be scattered into higher superbands. The numerical results presented below bear on this question.

We further assume

a)
$$E_1 = E_0 [1 - \cos(ak_{||})],$$
 (9)

where a is the superlattice constant,

b) scattering is either elastic or is inelastic with an energy change of one optical-mode quantum:

$$E' = E + s\hbar\omega_{o}; \ s = 0, \pm 1,$$
 (10)

 c) scattering matrix element is constant in either elastic or inelastic channel;

$$W(\mathbf{k}, \mathbf{k}') d^{3}\mathbf{k}' = (a/2\pi) dk_{\parallel}' dE_{2}' [A\delta(E - E') + BN_{0}\delta(E + \hbar\omega_{0} - E') + B(N_{0} + 1)\delta(E - \hbar\omega_{0} - E')],$$

where

$$N_{o} = \left[\exp(\hbar \omega_{o} / kT) - 1 \right]^{-1}$$
 (12)

and A, B are constants. The system of Eq. (1) with ε time-independent and Eqs. (4), (5), (9), (11) and (12) is physically consistent, embodying the detailed balance principle for a specific temperature T [4]. Its solution depends on the parameters $\hbar\omega_0/E_0$, kT/E_0 , $(h/a)A/e\,\varepsilon$, $(h/a)B/e\,\varepsilon$. It has been solved numerically for quantities of interest, as reported below, by Monte Carlo computation.

3. Steady-state calculation

The Monte Carlo programming was on lines that have been made familiar by Rees and his colleagues [5]. The total scattering rate including "self scattering" [5,6] was a constant, equal to

$$\Gamma = A + (2N_0 + 1) B. {(13)}$$

In a scattering event, a new k_{\parallel} value,

$$k_{\parallel}' = (2\pi/a) R,$$

was selected, where (here, and throughout) R is a pseudorandom number with constant probability density in (0, 1); and one of the three scattering modes in (10), with probabilities A/Γ , N_0B/Γ , and $(N_0+1)B/\Gamma$ for s=0, +1, and -1, respectively, was then chosen in the usual way with a new R. If the resulting new E_2 value

$$E_{2}' = E_{2} + s\hbar\omega_{0} + E_{1} - E_{1}' \tag{14}$$

was positive, the selected physical scattering process occurred; otherwise, there was a "self scattering." The acceleration path, generated by a new R, was an increase in $k_{||}$, equal to $(e \, \ell / \hbar \Gamma) \ln (1/R)$, with E_2 unchanged. After each trial the stored value of $(a k_{||})$ was replaced by its value mod (2π) .

An unusual feature of the programming was the use of the population of initial states in scatterings (final states in accelerations) as the ensemble that was averaged over, to obtain the expectations given by integrals over f [7]. That is,

$$\langle X \rangle \equiv \int X(\mathbf{k}) f(\mathbf{k}) d^3 \mathbf{k} = \frac{1}{L} \sum_{j=1}^{L} X(\mathbf{k}_b^{(j)}), \qquad (15)$$

Table 1 Parameter values and computation results.

		Input parameters in the computations								
(10^{-3}^{8}eV)	(10^7cm/s)	$\frac{kT}{E_0}$	$rac{\hbar\omega_{ m o}}{E_{ m o}}$	Â	Â	$\langle \hat{E}_{\rm 1} \rangle_{\rm 0}$	$\langle \hat{E}_{\scriptscriptstyle 2} \rangle_{\scriptscriptstyle \infty}$	$\frac{u_{\max}}{\mu_0 \mathcal{E}_{\max}}$	$\mu_0 \ \mathcal{E}_{\text{max}}$ (10^7 cm/s)	$\hat{ au}_{ ext{min}}$
		0.2	0.25	1.0	1.0	0.107	5.8	0.3		0.357
55	5.01	0.455	0.636	1.0	1.0	0.272	2.5	0.38	2.8	0.376
27.5	2.51	0.91	1.27	1.0	1.0	0.520	1.9	0.36	1.25	0.376
27.5	2.51	0.91	1.27	3.0	1.0	0.520	2.8	0.35	1.0	0.215
	55 27.5	55 5.01 27.5 2.51	$ \begin{array}{c c} E_{0} \\ (10^{-3^{0}} \text{eV}) & (10^{7} \text{cm/s}) \\ \hline & & & & \\ & & & & \\ & & & & \\ & & & & \\ & & & & $	$ \frac{E_{0}}{(10^{-30} \text{eV})} \qquad (10^{7} \text{ cm/s}) \qquad \frac{kT}{E_{0}} \qquad \frac{\hbar \omega_{0}}{E_{0}} $ $ 0.2 \qquad 0.25 $ $ 0.455 \qquad 0.636 $ $ 27.5 \qquad 2.51 \qquad 0.91 \qquad 1.27 $	$ \begin{array}{c ccccccccccccccccccccccccccccccccccc$	$\frac{E_0}{(10^{-30} \text{eV})} \qquad \frac{v_0}{(10^7 \text{ cm/s})} \qquad \frac{kT}{E_0} \qquad \frac{\hbar \omega_0}{E_0} \qquad \hat{A} \qquad \hat{B}$ $0.2 \qquad 0.25 \qquad 1.0 \qquad 1.0$ $0.455 \qquad 0.636 \qquad 1.0 \qquad 1.0$ $27.5 \qquad 2.51 \qquad 0.91 \qquad 1.27 \qquad 1.0 \qquad 1.0$	$\frac{E_0}{(10^{-30} \text{eV})} \frac{v_0}{(10^7 \text{ cm/s})} \frac{kT}{E_0} \frac{\hbar \omega_0}{E_0} \hat{A} \hat{B} \langle \hat{E}_1 \rangle_0$ $0.2 0.25 1.0 1.0 0.107$ $0.455 0.636 1.0 1.0 0.272$ $27.5 2.51 0.91 1.27 1.0 1.0 0.520$	$\begin{array}{c ccccccccccccccccccccccccccccccccccc$	$\frac{E_0}{(10^{-30} \text{eV})} \frac{v_0}{(10^7 \text{ cm/s})} \frac{kT}{E_0} \frac{\hbar \omega_0}{E_0} \hat{A} \hat{B} \langle \hat{E}_1 \rangle_0 \langle \hat{E}_2 \rangle_{\infty} \frac{u_{\text{max}}}{\mu_0 \mathcal{E}_{\text{max}}}$ $\frac{0.2}{55} \begin{array}{cccccc} 0.25 & 1.0 & 1.0 & 0.107 & 5.8 & 0.3 \\ 0.455 & 0.636 & 1.0 & 1.0 & 0.272 & 2.5 & 0.38 \\ 27.5 & 2.51 & 0.91 & 1.27 & 1.0 & 1.0 & 0.520 & 1.9 & 0.36 \\ \end{array}$	$ \frac{E_0}{(10^{-30} \text{eV})} \frac{v_0}{(10^7 \text{ cm/s})} \frac{kT}{E_0} \frac{\hbar \omega_0}{E_0} \hat{A} \hat{B} \langle \hat{E}_1 \rangle_0 \langle \hat{E}_2 \rangle_\infty \frac{u_{\text{max}}}{\mu_0 \mathcal{E}_{\text{max}}} \frac{\mu_0 \mathcal{E}_{\text{max}}}{(10^7 \text{cm/s})} $

where X is any function of electron state, the subscript b refers to the state immediately preceding a scattering (either "self" or physical), the index j signifies the jth trial, and L is the number of trials in the Monte Carlo "history."

Natural reduced variables in the calculations are

$$\hat{k} = ak_{||}, \tag{16}$$

$$\hat{E}_{1,2} \equiv E_{1,2}/E_0, \quad \hat{E} \equiv E/E_0$$
 (17)

with the parameters kT/E_0 , $\hbar\omega_o/E_0$. A set of such variables, which has been used both in the computer program and in presenting the results here, is obtained by introducing an arbitrary constant, ρ , with the dimensions of a frequency. Then

$$\hat{\varepsilon} = \varepsilon \left(ea/\hbar \rho \right), \tag{18}$$

$$\hat{A} \equiv A/\rho, \quad \hat{B} \equiv B/\rho \ . \tag{19}$$

The velocity in the field direction, by (3) and (9), is

$$v_{\parallel} = v_0 \sin \left(ak_{\parallel} \right) \,, \tag{20}$$

where

$$v_0 = aE_0/\hbar . (21)$$

Our reduced drift velocity is then

$$\hat{u} = u/v_o. \tag{22}$$

The differential mobility (calculated as described in Section 4) depends on the frequency, ν , which we specify by a reduced frequency

$$\hat{\nu} \equiv \nu/\rho \,. \tag{23}$$

It is not useful to specify drift velocity versus field, for example, in absolute units, because the results scale homogeneously in field and frequency (reciprocally in time). When the quantities in (21) are given, the fields could be normalized by a value for the actual ohmic mobility μ_0 relative to v_0 .

Results are presented here for the cases specified in Table 1. Case III corresponds to temperature T = 290 K; optical mode quantum $\hbar\omega_0 = 0.035 \text{ eV}$; and the specu-

lative estimate [2], for the lowest superband width, $2E_0 = 0.055$ eV. The v_0 value comes from (21) with [2] an assumed superlattice constant $a = 6 \times 10^{-7}$ cm. Case IV is the same as III except for a value of \hat{A} three times as large (that is, three times as much elastic scattering). Case II is the same as III except for having twice the superband width. Case I represents the situation of even larger bandwidth, and somewhat smaller $\hbar\omega_0$, by the "round number" values that are assumed for kT/E_0 , $\hbar\omega_0/E_0$.

Figures 1-5 show results for the steady state. Reduced drift velocity versus reduced field (Figs. 1-4) is of the expected form. From the initial ohmic mobility, μ_0 , the maximum drift velocity, $u_{\rm max}$, and the field at the maximum, $\varepsilon_{\rm max}$, we form the dimensionless quantity $u_{\rm max}/\mu_0$ $\varepsilon_{\rm max}$ given in Table 1 (actually calculated from the three reduced values). These values, between 0.3 and 0.4, compare with the value 0.5 given by the formula

$$u = \mu_0 \varepsilon / [1 + (\varepsilon / \varepsilon_{\text{max}})^2]$$
 (24)

obtained by Esaki and Tsu [1]. Absolute fields could be established by equating $\mu_0 \, \hat{\epsilon}_{\max}$ to $v_0 \hat{\mu}_0 \, \hat{\epsilon}_{\max}$, the values being given in Table 1.

The general dependence of the energy averages, $\langle E_1 \rangle$ and $\langle E_2 \rangle$, on field, illustrated in Figs. 1-3, is as expected. The zero-field limit of $\langle E_1 \rangle$ in general exceeds $\frac{1}{2}kT$, as it should: The energy function (9) gives, for a Boltzmann thermal distribution,

$$\langle \hat{E}_1 \rangle_0 = 1 - I_1 (E_0/kT) / I_0 (E_0/kT) ,$$
 (25)

where the $I_n(x)$ are Modified Bessel Functions [8]. This expression goes from $kT/2E_0$ in the limit $T \to 0$ to one in the limit $T \to \infty$. It is displayed in Fig. 6, and the applicable values are given in Table 1. The high-field limit of $\langle \hat{E}_1 \rangle$ is one, in accordance with (6). Figure 5 shows, for Case III, the distribution function of $k_{||}$ at two intermediate fields; the progressive flattening of the distribution, towards the ultimate uniformity in $k_{||}$ at large fields, is apparent.

The averages $\langle E_2 \rangle$ start at the thermal value kT for zero field and increase to limiting high-field values, which

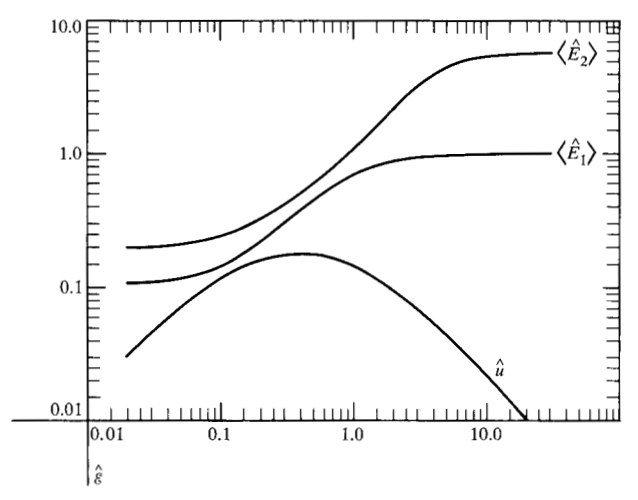
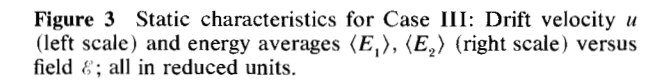
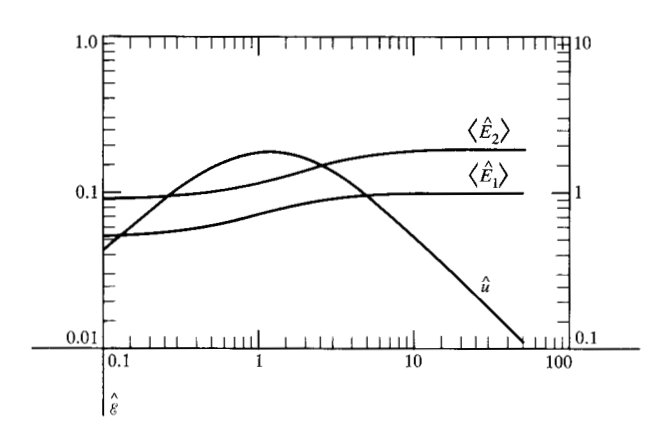


Figure 1 Static characteristics for Case I: Drift velocity u and energy averages $\langle E_1 \rangle, \langle E_2 \rangle$ versus field ε ; all in reduced units.





are given in Table 1 as $\langle \hat{E}_2 \rangle_\infty$. The evident trend is a decreasing $\langle \hat{E}_2 \rangle_\infty$, and hence a more strongly decreasing $\langle E_2 \rangle_\infty$, with decreasing E_0 at fixed temperature and optical mode frequency. (On the other hand, increasing the proportion of elastic to inelastic scattering resulted in a larger high-field $\langle E_2 \rangle$.) This indicates that increasing strength of the superlattice potential (greater height or width of the barrier [1]) goes with more effective exclusion of the hot carriers from the superlattice bands above the lowest. The distribution function for E_2 was found to be Maxwellian (but with a temperature greater than T) in all of the many cases examined. This characteristic was not investigated analytically. For Case III, the bottom of the second superband has been calculated [2] to be 2.9 E_0 above the bottom of the lowest superband. The

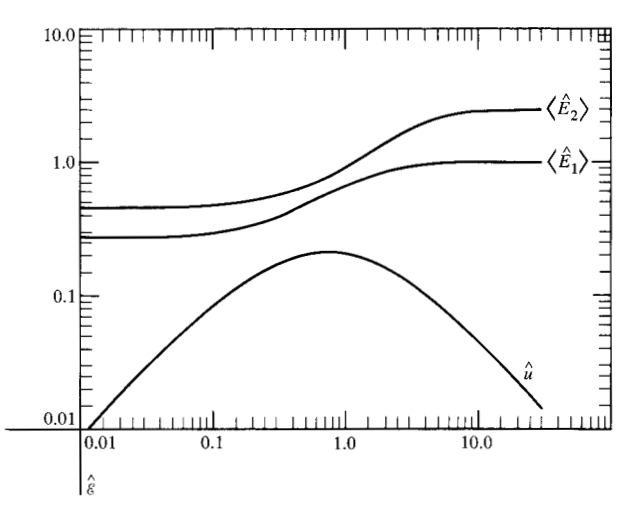
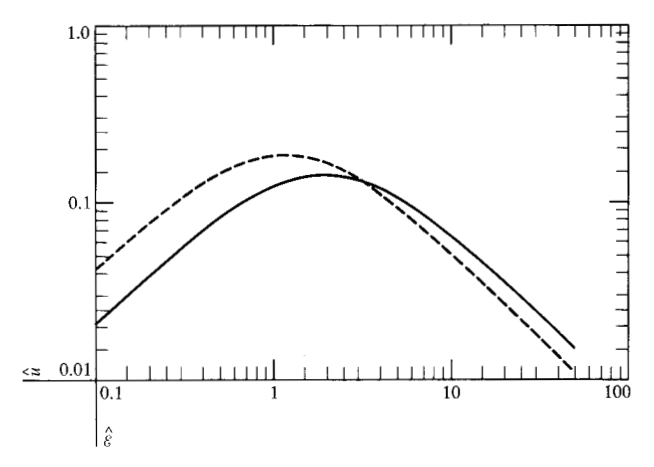


Figure 2 Static characteristics for Case II: Drift velocity u and energy averages $\langle E_1 \rangle$, $\langle E_2 \rangle$ versus field \mathcal{E} ; all in reduced units.

Figure 4 Drift velocity versus field for Case IV (full curve), compared with Case III (dashed curve); all in reduced units.



proportion of carriers with energies greater than this, according to the calculations presented here, would be $\exp(-2.9/1.2) = 0.089$ at ε_{\max} ; and $\exp(-2.9/1.9) = 0.22$ at the high-field limit.

It would be of interest, in the light of the foregoing, to repeat the calculations of this section and the following one with addition of the next higher superband to the model. One would expect the results to be sensitive to the energy parameters and relative scattering rates, however; and there evidently is not, at present, an adequate basis for assigning values to these. Tunneling between superbands, possibly a source of appreciable additional current, is of course outside the scope of the quasi-classical formulation on which the present calculations are

4. Differential mobilities

The quantities of interest next after the static drift velocity u, versus field \mathcal{E} , are the differential mobilities that give the response to a small superposed harmonically varying field; that is, the coefficients $\mu_1(\nu)$ and $\mu_2(\nu)$, which give the additional drift velocity

$$\delta u = (\mu_1 \sin 2\pi \nu t + \mu_2 \cos 2\pi \nu t) \, \varepsilon_{\nu}$$

$$\equiv u_1 \sin 2\pi \nu t + u_2 \cos 2\pi \nu t \tag{26}$$

due to the additional field

$$\delta \, \varepsilon = \varepsilon_{\nu} \sin 2\pi \nu t \,. \tag{27}$$

The basic idea, for obtaining these coefficients by a refinement of the usual Monte Carlo procedure, is to use a time-varying field $\mathcal{E}(t)$, by addition of (27) to the static term, in calculating the "path" steps in the Monte Carlo history; and to extract from the latter the corresponding Fourier components of the electron velocity over time. With a constant total scattering rate (including "self scattering") the scattering events are not correlated with the phase in (27). The intervals between scatterings are still given by

$$t^{(j+1)} - t^{(j)} = (1/\Gamma) \ln(1/R)$$
, (28)

and the path increments of wavevector by integration of

$$dk_{\parallel}/dt = (e/\hbar) \ \mathcal{E}(t) \ . \tag{29}$$

In the present case, the integral of (29) includes a term $(e/\hbar) (\mathcal{E}_{n}/2\pi\nu) (\cos 2\pi\nu t^{(j)} - \cos 2\pi\nu t^{(j+1)})$.

The coefficients in (26) are equal to the time averages of $2 v_{||} \sin{(2\pi\nu t)}$ and $2 v_{||} \cos{(2\pi\nu t)}$ over the Monte Carlo history. Given the functional dependence v(k), the time integrals over paths, which are summed to give an average, may be expressed in terms of the k values at the path ends (the initial and final states of the scatterings). Alternatively, however, one may, in the present case also, replace the explicit time averages by averages over final path states as in (15). Lebwohl [9] has demonstrated the equivalence of the two procedures and has verified it numerically for the case of several valleys with "parabolic" energy functions. Even for the latter case, and much more so for the present one with the energy function (9), the procedure corresponding to (15) is simpler. We take

where $\theta = 2\pi vt = 2\pi \hat{v}t$.

An important feature of the results that were obtained, and are displayed in the corresponding Figures, is the

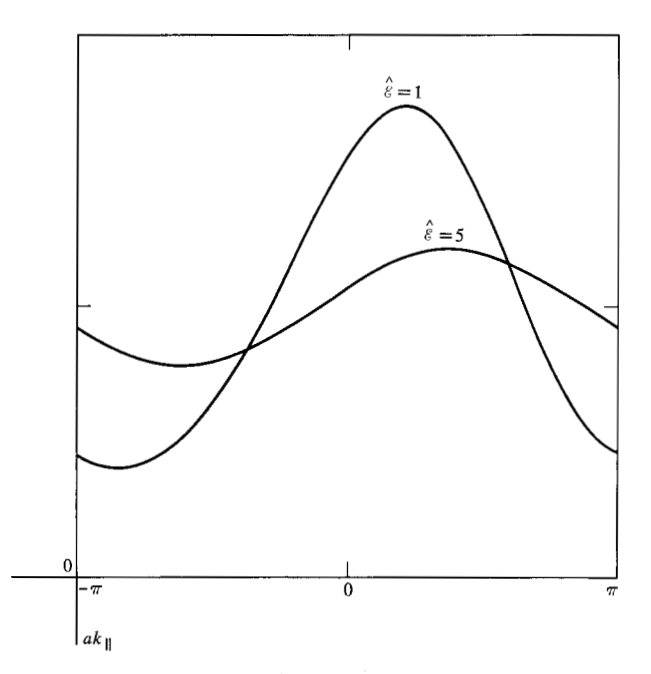
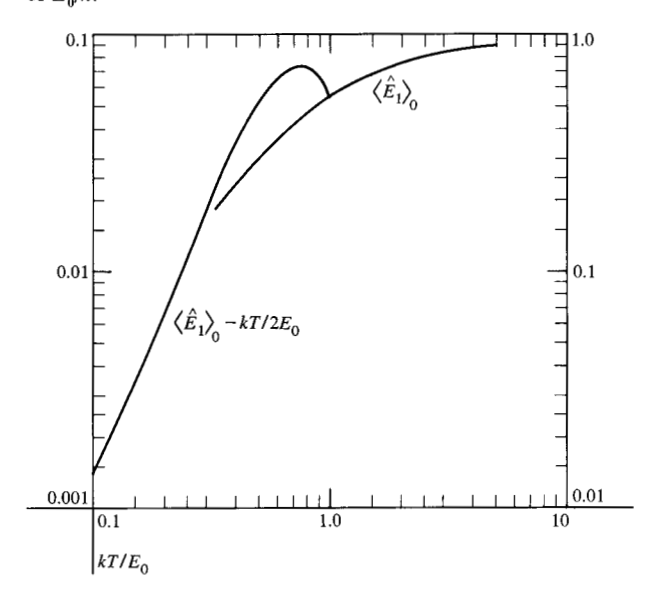


Figure 5 Distribution function of ak_{\parallel} , for Case III, at the reduced field values labelling the curves.

Figure 6 Thermal average value of E_1 (right scale) and of $(E_1 - \frac{1}{2k}T)$ (left scale), both in units of E_0 , versus T in units of E_0 .



"Bloch resonance." In a static field ε , an unscattered electron crosses the Brillouin super-zone in a time $(2\pi/a)(\hbar/e \varepsilon)$. One therefore expects an enhanced response to the superposed field (27) when the frequency is near the reciprocal of this transit time; that is, when the reduced frequency is near

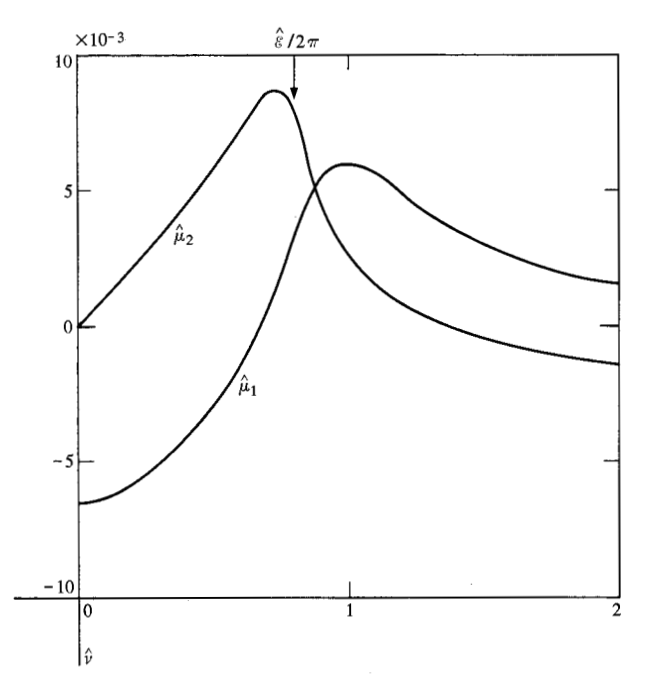
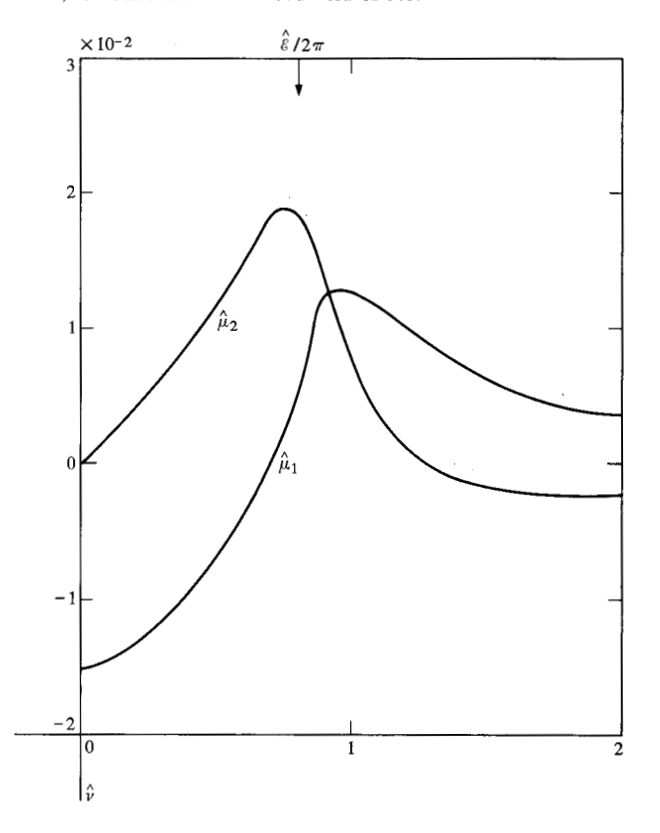


Figure 7 Differential mobilities versus frequency, in reduced units, for Case I at a reduced field of 5.0.

Figure 8 Differential mobilities versus frequency, in reduced units, for Case II at a reduced field of 5.0.



$$\hat{\nu}_{\rm B} = \hat{\varepsilon} / 2\pi \,. \tag{31}$$

This "Bloch frequency" is indicated by an arrow on each of Figs. 7-10.

The frequency range of this enhanced response might be expected to approximate the physical scattering rate. The latter is not a unique quantity in the present case; but it does have a maximum value, in the band, equal to the total scattering rate Γ given by (13). The reciprocal of Γ in reduced units,

$$\hat{\tau}_{\min} = \rho/\Gamma \,, \tag{32}$$

is given for each Case in Table 1. The corresponding " $\omega \tau$ " is equal to $\hat{\tau}_{\min}$ $\hat{\varepsilon}$ for the particular field.

Figures 7-10 show differential mobilities versus frequency, in reduced units. In each case, the curve that starts at the origin (0,0) is for μ_2 . Figure 7 is for Case I, with $\hat{\ell}=5.0$; the minimum " $\omega\tau$ " value that applies is 1.8. Figures 8 and 9 are for Case II. The reduced field and minimum " $\omega\tau$ " values are, respectively, 5.0 and 1.9 for Fig. 8; 0.5 and 0.19 for Fig. 9. Figure 10 is for Case III, with $\hat{\ell}=2.5$ and minimum " $\omega\tau$ " equal to 0.94. A convincing resonance structure appears, at about the right place, in each case. From Figs. 8 and 9 it is evident that the position of this structure shifts with field as it should according to (31).

Although the zero-frequency value of μ_1 is positive or negative according to the sign of $du/d\varepsilon$ at the static field value, the resonance maximum of μ_1 is positive in all these cases. Thus the negative-differential-mobility property shown by the static $u(\varepsilon)$ is actually obliterated, not enhanced, by resonance conditions. It is noteworthy that $d\mu_2/d\nu$ is positive, for either sign of μ_1 , at zero frequency; this is contrary to what was found for GaAs, as a transferred-electron system, by Rees [10].

The ε_{ij} value used in obtaining these data was in each case 0.2 times the static-field value. A test of the linearity of the response was made for the case of Fig. 10, at $\hat{\nu}$ = 0.4 (in the resonance region), by plotting u_1 and u_2 versus \mathcal{E}_{v} . For u_1 the deviations from proportionality occurred well above the value $\hat{\varepsilon}_{\nu} = 0.5$ that had been used; and for u_2 significantly above it; and the μ_1 and μ_2 that had been derived were both good values on the proportionality lines. It was found that the static averages ("zero-frequency components") of v_{\parallel} , E_1 and E_2 , especially the first of these, were similarly sensitive to the added sinusoidal field amplitude \mathcal{E}_{ν} , so that deviations from their values with the static field alone were good indicators of nonlinearity in δu . A check of the values for the computer runs from which Figs. 7-10 were obtained showed some deviations of a percent or two, but not more serious ones. Evidently there were μ_1 and μ_2 data points from somewhat beyond the perceptible range of linearity; but I do not believe that the results presented are significantly inaccurate from this source.

A consequence of (1) is that the high-frequency limit of μ_2 is inversely proportional to the frequency:

$$2\pi \lim_{n \to \infty} (-\mu_2 \nu) = C \tag{33}$$

with

$$C = e\langle 1/m_{||} \rangle \equiv e\langle (1/\hbar^2) d^2 E/dk_{||}^2 \rangle.$$
 (34)

Then, from (9) and (34), we have (in reduced units, for convenience)

$$\hat{C} = 1 - \langle \hat{E}_1 \rangle. \tag{35}$$

A necessary analytical property, in relation to (33), is [11]

$$4\int_{0}^{\infty} \mu_{1} \ d\nu = C \ . \tag{36}$$

A rather careful check of the numerical agreement of these formulas was made for the case of Fig. 9, with the following results:

$$2\pi \lim_{\nu \to \infty} (-\hat{\mu}_2 \hat{\nu}) = 0.53$$
,

$$1 - \langle \hat{E}_1 \rangle = 0.52 ,$$

$$4\int_0^\infty \hat{\mu}_1 \ d\hat{\nu} = 0.49 \ .$$

The integral was actually evaluated for an upper limit $\hat{\nu}=2.0$, where μ_1 has evidently dropped to zero. The substantial "exhaustion of the sum rule" within this frequency range supports the conclusion that there are no resonances at harmonics of the fundamental Bloch frequency. The relation

$$\mu_1(0) = -\frac{2}{\pi} \int_0^\infty \frac{\mu_2}{\nu} \, d\nu \tag{37}$$

is companion to (33), (36). This is also available for a check of results for differential mobility versus frequency.

To obtain this quantity of differential-mobility results required quite a lot of computer time—though without any special effort at efficient estimators. The requirement seems to be essentially a matter of "signal-to-noise" for (30); this is discussed in the Appendix.

5. Discussion

What has been done in this paper is to adopt a reasonable and consistent model of the semiconductor superlattice, using a single-particle space-homogeneous quasi-classical treatment; show for this model that the static and linear differential transport properties can be calculated with precision; and obtain enough numerical results to give what seems to be a quite good idea of those properties. More of such data could, of course, be obtained as desired. What might be more useful, and obviously is possible, is to investigate in detail the beyond-linear dif-

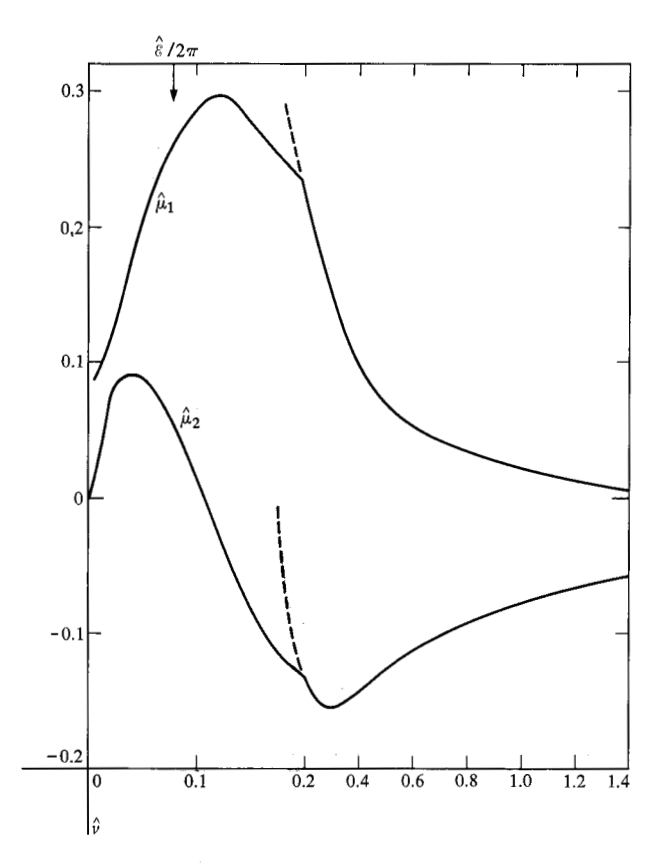
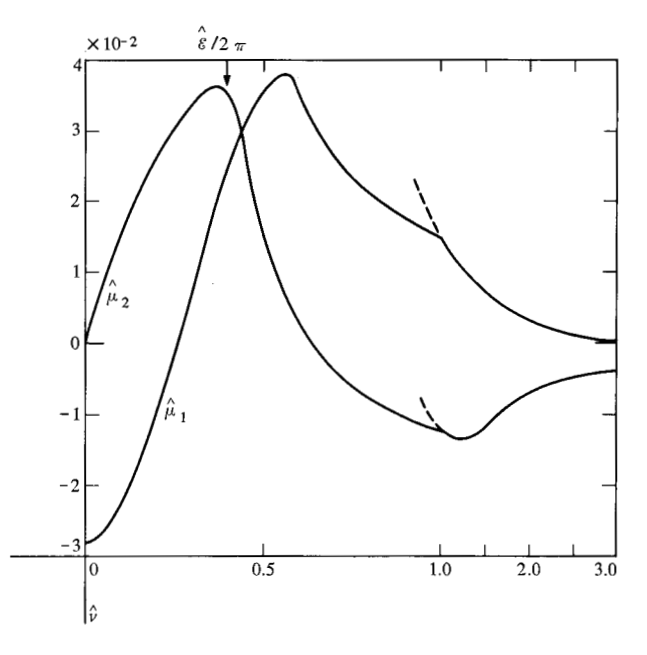


Figure 9 Differential mobilities versus frequency, in reduced units, for Case II at a reduced field of 0.5. The frequency scale changes at 0.2.

Figure 10 Differential mobilities versus frequency, in reduced units, for Case III at a reduced field of 2.5. The frequency scale changes at 1.0.



ferential response for large amplitudes. The practical interest, for these highly non-parabolic electron band systems, is obvious. There should also be a more fundamental interest in verifying theorems such as the generalization of Eqs. (34) and (36); and perhaps the generalization of the Kramers-Kronig relations [12].

It seems plausible that, just as with Gunn domains, an understanding of observed properties will require a many-particle treatment with space and time dependence, incorporating space-charge and dynamical instability phenomena. This development could, however, be based on the same physical model as for the present paper. The physics of superlattice materials is, of course, a broader subject than this model comprises.

Appendix. Fluctuations of the differential mobility estimator

The characteristic fluctuations of the estimator (30) may be analyzed, after replacing it by the equivalent time average, by the identity that is the basis of the Weiner-Khinchine theorem: If

$$\tilde{X}(T,\nu) \equiv \int_{-\frac{1}{2}T}^{\frac{1}{2}T} X(t) \exp(i2\pi\nu t) dt$$
 (A1)

and similarly for Y, then

$$\tilde{X}(T,\nu)\tilde{Y}(T,-\nu) = \int_{-\infty}^{\infty} ds \, \exp(i2\pi\nu s)$$

$$\int_{s\to t}^{\frac{1}{2}T} X(t+s)Y(t) \, dt \,. \tag{A2}$$

If, now, X(t) and Y(t) are fluctuating quantities with (for either or both) average value equal to zero, and if T is large compared to their correlation time, the second integral in (A2) may be replaced by T times the correlation at time displacement s. That is, in the usual notation, for large T

$$\tilde{X}(T, \nu)\tilde{Y}(T, -\nu)$$

$$= T \int_{-\infty}^{\infty} \exp(i2\pi\nu s) \, \overline{X(t+s)Y(t)} \, ds \,. \tag{A3}$$

Thus, for large T

$$\frac{1}{T} \left(\int_0^T dt \ v(t) \left\{ \sin 2\pi \nu t \right)^2 \right.$$

$$= \int_0^\infty ds \cos(2\pi \nu s) \ \overline{[v(t) - u]v(t+s)}$$
 (A4)

(where either or both factors in the correlation average on the right could be v-u rather than v). The right-hand side of (A4) is the diffusivity at frequency v. The left-hand side may be written as $T(\Delta v)^2$, where Δv is the fluctuation at frequency v which occurs in the sample "history" of duration T; and the right-hand side may be written as $\langle v^2 \rangle \tau_c$, where τ_c is the effective correlation time at frequency v. Replacing T by L/Γ , where L is the number of trials in the Monte Carlo run, we have

$$\Delta v = (\langle v^2 \rangle \Gamma \tau_c / L)^{\frac{1}{2}}. \tag{A5}$$

In the present case, it follows from (8) and (20) that $\langle v^2 \rangle$ is less than $v_0^2 \langle \hat{E}_1 \rangle$ (2 $-\langle \hat{E}_1 \rangle$) and hence is less than v_0^2 . On the other hand δu , the amplitude to be measured, is (in the work presented here) of order u/10; and u is characteristically of order $v_0/10$. So we may write

$$\frac{\Delta v}{\delta u} \lesssim \frac{100}{\sqrt{L}} \cdot \sqrt{\Gamma \tau_{\rm c}} \,. \tag{A6}$$

Where $\hbar\omega_0$ is not much smaller than E_0 , especially, we don't expect $\Gamma\tau_c$ to be large. Without investigating further, we conclude that probably $\Delta v/\delta u$ does not much exceed $100/\sqrt{L}$. In practice, in the work reported here, this conclusion turns out to be somewhat on the pessimistic side.

References and notes

- 1. L. Esaki and R. Tsu, IBM J. Res. Develop. 14, 61 (1970).
- L. Esaki, private communication. The most recent publication is L. Esaki, L. L. Chang, W. E. Howard and V. L. Rideout, "Transport Properties of a GaAs-GaAlAs Superlattice," to be published in the Proceedings of the 11th International Conference on Semiconductor Physics, Warsaw, 1972. The text of the paper is currently available as IBM Research Report RC3940, Yorktown Heights, New York.
- 3. This is not the sole condition for the application of a quasiclassical formulation, in this case to the "Bloch" states of the superlattice. See, for example, P. J. Price, *IBM J. Res. Develop.* 10, 395 (1966), and references therein.
- 4. The theoretical analysis given in Ref. 1 implicitly assumes, with a constant physical scattering rate, a scattering function in which the distribution of final states for any given initial state is a thermal Boltzmann distribution (and the actual calculations further assume that $kT \ll E_0$). Such a model is physically consistent, and is attractive because an exact analytical treatment of the transport properties can be made; but it is hardly realistic, in respect of the characteristic energy changes in scattering.
- A. D. Boardman, W. Fawcett and H. D. Rees, Solid State Comm. 6, 305 (1968); W. Fawcett, A. D. Boardman and S. Swain, J. Phys. and Chem. Solids 31, 1963 (1970).
- 6. H. R. Skullerud, J. Phys. D 1, 1567 (1968).
- P. J. Price, Bull. Am. Phys. Soc. 16, 123 (1971), abstract GG4.
- M. Abramowitz and I. Stegun, eds., Handbook of Mathematical Functions, National Bureau of Standards, 1964.
- 9. P. A. Lebwohl, J. Appl. Phys., in press.
- 10. H. D. Rees, *IBM J. Res. Develop.* 13, 537 (1969), see Fig. 6.
- 11. See pages 378-9 in Chapter 8 of R. E. Burgess, ed., Fluctuation Phenomena in Solids, Academic Press, 1965. The appearance of the superband (or band) differential mass, rather than the free electron mass, on the right of (34), (36), is an artifact of the quasi-classical model. It corresponds to a frequency range that would not, in physical reality, extend to infinity.
- 12. P. J. Price, Phys. Rev. 130, 1792 (1963).

Received September 5, 1972

The author is located at the IBM Thomas J. Watson Research Center, Yorktown Heights, New York 10598.